FULL PAPER

Extracellular Microreactor for the Depletion of Phenylalanine Toward Phenylketonuria Treatment

Leticia Hosta-Rigau, Maria J. York-Duran, Tse Siang Kang, and Brigitte Städler**

Phenylketonuria (PKU) is a genetic enzyme defect affecting 1:10 000–20 000 newborn children every year. The amino acid phenylalanine (Phe) is not depleted but accumulates in tissues of several organs, which leads to severe medical conditions. A promising concept to restore the metabolism of the affected patients will be to orally administer the defective enzyme which will remove Phe in the intestine. Herein, capsosomes, a multicompartment carrier consisting of thousands of liposomes embedded within a polymeric carrier, are employed as encapsulation platform for this purpose. It is shown that the enzyme phenylalanine ammonia lyase can be entrapped within the liposomal compartments with preserved activity, demonstrated by the conversion of Phe into *trans*-cinnamic acid (*t*-ca). With the aim to mimic the dynamic environment in the intestine, the Phe conversion is performed in a microfluidic set up in the presence of human intestinal epithelial cells with applied intestinal flow and peristaltic motions. It is also shown that the microreactors are neither internalized by the cells nor exhibit inherent cytotoxicity while concurrently converting Phe into *t*-ca. Taken together, the first active extracellular multicompartment microreactor is reported using the relevant enzymes and settings toward the treatment of the medical condition PKU.

1. Introduction

Phenylketonuria (PKU) is the most common genetic enzyme defect, with an overall incidence in Europe and the USA of 1:10 000–20 000 live births per year.[1] Patients suffer from a genetic defect in the liver enzyme phenylalanine hydroxylase (PAH), which normally metabolizes the amino acid (AA) phenylalanine (Phe) into the AA tyrosine. This specific enzyme defect, which results in an increase in the level of systemic Phe in the first years of life, can lead to severe mental retardation, microcephaly, and seizures.[2] The implementation of newborn screening to detect PKU has facilitated the early use of a dietary treatment to reduce the Phe uptake. Dietary treatment has been the cornerstone for controlling systemic Phe levels in PKU for the past four decades, but the diet can be very difficult to maintain. Therefore, alternative approaches of therapy are being pursued.[2,3] Current strategies for the treatment of PKU are either based on enzyme or gene therapy.[2] However, so far, gene therapy has only been employed with limited success due to poor efficiency of gene delivery into the liver and lack of sustained gene expression.[4] Thus, enzyme therapy is currently the most promising concept. The nonhuman enzyme phenylalanine ammonia lyase (PAL) which can be readily obtained from plants, some fungi, yeasts, and E. *coli*,[2,5] converts Phe into nontoxic *trans*-cinnamic acid (*t*-ca) which is subsequently converted in the liver to benzoic acid secreted via urine.[5b,6]

Although many studies have been carried out on the use of enzyme therapy for replacing defective enzymes,[7] the systemic delivery of enzymes and proteins in general possesses a number of problems and risks. Enzymes are rapidly degraded in the bloodstream, which makes them difficult to reach their site of action and remain active for a sufficient amount of time.[8] On the other hand, the administration of therapeutic enzymes via the oral route, a more convenient administration pathway for pediatric patients, remains challenging due to potential inactivation of these fragile macromolecular entities in the harsh environment of the gastrointestinal (GI) track.[9] For PKU treatment, PAL is an ideal candidate to be administered orally, since the optimal pH of PAL are 8.75 (PAL from *Rhodotorula glutinis*)[10] and 8.0 (PAL from *Rhodotorula rubra*),[11] which are close to the average pH of the small intestine. Additionally, the depletion of intestinal Phe by the administered enzyme could significantly lower the plasma Phe levels.[12] Although the levels of AA in the intestine are many times higher than those of the body fluids, it has been demonstrated than most of the AA of the intestine do not come from ingested food,[12] thus making possible to orally administer enzymes to remove/convert an specific AA.[13] However, due to the aforementioned challenges, the concept of oral enzyme replacement therapy has been around for some time with only a small degree of success,[9] and a number of stabilization strategies[14] such as functional modifications of PAL with poly(ethylene glycol) which altered the catalytic properties of the enzyme[15] or formulation approaches[16] like the encapsulation

Dr. L. Hosta-Rigau, M. J. York-Duran, Dr. B. Städler
Interdisciplinary Nanoscience Centre (iNANO)
Aarhus University
Gustav Wieds Vej 14, 8000, Denmark
E-mail: leticia@inano.au.dk; bstadler@inano.au.dk
Dr. T. S. Kang
Department of Pharmacy
National University of Singapore
18 Science Drive 117543, Singapore

DOI: 10.1002/adfm.201404180

of lactase in microcapsules which proved to be quite instable in the gastric environment,[17] have been investigated.

An alternative approach to overcome the shortcomings of enzymatic replacement therapy will be the protection of the enzyme using an advanced encapsulation platform. The development of artificial cells, which consist of carriers containing multiple compartments with a structure reminiscent of a biological cell, is an approach that aims to substitute for missing or lost cellular function, often in the context of enzyme replacement therapy.[18] We recently developed capsosomes, which consist of liposomes embedded within a polymer carrier capsule.[19] In such a biomedical platform, biological active materials (e.g., enzymes) can be trapped within the liposomal compartments. Liposomes are ideal candidates to encapsulate fragile (large) biomolecules, such as enzymes, protecting them from misfolding or denaturation while small molecules can cross the lipid bilayer. However, liposomes have some limitations such as low stability and fast degradation in biological fluids. On the other hand, the polymeric carrier provides the required structural integrity and the semipermeable nature of the polymer membrane allows for the controlled exchange of (relatively large) molecules between the carrier's interior with the external milieu. By using such a microreactor, the encapsulated enzyme will be prevented from coming into direct contact with degrading external entities present in the GI track such as tryptic enzymes, since PAL has been reported to be to be degraded by both trypsin and chymotripsin.[20] The microreactors will be moving through the stomach, reaching the intestine where they will act as an enzyme bioreactor removing the unwanted substrate (Phe).

Herein, we report the assembly of PAL-loaded core-shell particles and capsosomes (**Scheme 1**a), and we demonstrate their use as extracellular microreactors for the depletion of Phe toward the treatment of PKU. Specifically, we (i) demonstrate that encapsulated PAL enzymes within poly(dopamine)-based capsosomes are able to repeatedly convert Phe into *t*-ca (ii) assess the stability over time of PAL-loaded microreactors (capsosomes with or without core) for storage purposes, (iii) evaluate the interaction of the microreactors with human intestinal epithelial cells with applied peristaltic flow simulating the dynamic environment in the intestine, and (iv) demonstrate that PAL-loaded microreactors are able to conduct an enzymatic reaction in the presence of intestinal epithelial cells after and while being exposed to peristaltic flow.

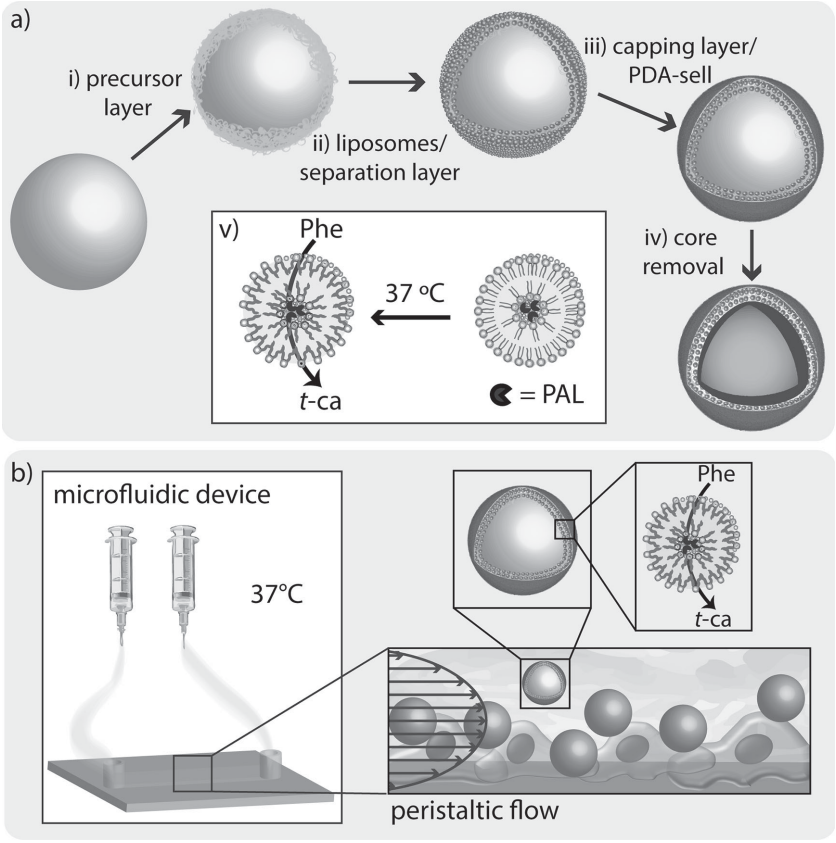

Scheme 1. a) Microreactor assembly. (i) A precursor poly(L-lysine) (PLL)/ poly(methacrylic acid)-*co*-(cholesteryl methacrylate) (PMA_c) polymer layer is deposited onto silica particles followed by the (ii) deposition of enzyme loaded liposomes and a separation polymer layer (PMA_c). (iii) The assembly is capped with a PMA_c polymer layer and the poly(dopamine) (PDA) shell is assembled in a single, solution-step procedure. If desired, the core is removed (iv) to obtain capsosomes. (v) Upon increasing the temperature to 37 °C ($T > T_m$), the substrate phenylalanine (Phe) is able to permeate through the liposome membrane, to interact with the encapsulated enzyme PAL and to be converted into *trans*-cinnamic acid (*t*-ca). b) Schematic representation of the employed microfluidic setup. Cell media containing Phe was loaded into a syringe attached to a pumping system and connected to a perfusion chamber with pre-cultured human intestinal epithelial cells and the desired amount of microreactors. The physiological peristaltic motions (peristaltic flow) in the intestine is mimicked by applying a low shear stress (0.24 dyn cm^{-2}) and a cyclic strain (0.15 Hz).

2. Results and Discussion

2.1. Characterization of PAL-Containing Capsosomes

2.1.1. Kinetics of the Encapsulated Enzymatic Reaction

An encapsulation platform is needed to preserve the activity of PAL when exposed to biological fluids. The approach is based on our recently reported poly(dopamine) (PDA)-based capsosomes, which consisted of liposomes embedded within a PDA carrier capsule.[21] While in most of our previous reports on functional capsosomes, crosslinked poly(methacrylate) deposited via the LbL technique was used for the carrier capsules,[22] the single-step deposition of PDA considerably facilitates the assembly of this part of the microreactors. We demonstrated that the function of capsosomes was not impeded by the different carrier capsules by co-encapsulating three different enzymes and confirming their simultaneous activity.[21] Herein, we aimed to advance the

applicability of capsosomes toward a medically relevant condition, namely the oral treatment of PKU. In order to achieve this goal, multiple research challenges have to be addressed such as improving the enzyme encapsulation efficiency of capsosomes by replacing the liposome subunits by polymersomes, characterize the structural and functional stability of the microreactors in the GI environment, or the removal of Phe in the intestine taking the presence of cells and the peristalsis-like movement of the small intestine into consideration. The current report focuses on the latter aspect, while the former aspects will be addressed in detail in a separate publication. In a first step, we encapsulated the PAL enzyme in the liposomal subunits of capsosomes and tested the enzymatic activity of the microreactors by converting the substrate Phe into *t*-ca (Scheme 1a, inset). To obtain capsosomes which are only active close to body temperature (≈37 °C), liposomes with a phase-transition temperature (T_m) in this range consisting of a mixture of the saturated zwitterionic lipids 1,2-dimyristoyl-*sn*-glycero-3-phosphocholine (DMPC, T_m = 24 °C) and 1,2-dipalmitoyl-*sn*-glycero-3-phosphocholine (DPPC, T_m = 41 °C) were employed.[22d] At room temperature (RT, 23 °C < T_m), the saturated liposomes provide an effective sealed barrier for small substrates. Upon increasing the temperature to or above the T_m of the liposomes (≈37 °C), the substrate Phe will be able to cross the lipid membrane and be converted into the product *t*-ca before being released from the compartment again (**Figure 1**a-i). The PAL-containing microreactors were assembled in tris(hydroxymethyl)aminomethane (TRIS) buffer (100×10^{-3} M, pH 7.0) by adsorbing two precursor polymer layers (poly-L-lysine (PLL) and poly(methacrylic acid)-*co*-(cholesteryl methacrylate) (PMA_c) onto 5 µm SiO_2 particles, followed by the adsorption of the first liposome layer. Prior to the addition of the second liposomes layer, a separation PMA_c layer was deposited. The assembly was capped with a PMA_c layer and the PDA carrier capsule was assembled in a single step by incubating the coated SiO_2 particles in a solution of dopamine (10×10^{-3} M) in TRIS buffer (pH 8.5). After 16 h of incubation, if desired, the core (silica particle) was removed using a 2 M HF/8 M ammonium fluoride (NH_4F) solution at pH 5. The structural integrity of the yielded capsosomes (without core) was verified by differential interference contrast (DIC) microscopy images. Figure 1a-ii demonstrates that the capsosomes were intact, discrete, nonaggregated and maintained the round shape of the template silica particles. The PAL-loaded capsosomes were incubated at RT and at 37 °C in a solution of 6×10^{-6} M Phe in phosphate buffer (10×10^{-3} M, pH 8.0), and the kinetics of the enzymatic reaction was followed using High Performance Liquid Chromatography (HPLC) by identifying the *t*-ac product at λ = 270 nm. Enzymatic conversion was only observed for capsosomes incubated at 37 °C, but not at RT (Figure 1b, black and white squares, respectively), and only in the presence of Phe (Figure 1b, black and white triangles, respectively). The results were normalized to the *t*-ca HPLC peak height after 24 h of the reaction for capsososmes incubated at 37 °C. The *t*-ca peak height at 270 nm steadily increases for all the measured time points and the capsosomes preserved their structural integrity after 24 h of reaction (Figure 1b, inset). These results not only confirmed the preserved activity of the enzyme, but they also showed that the enzyme was entrapped within intact liposomes due to the temperature dependence of the enzymatic conversion.

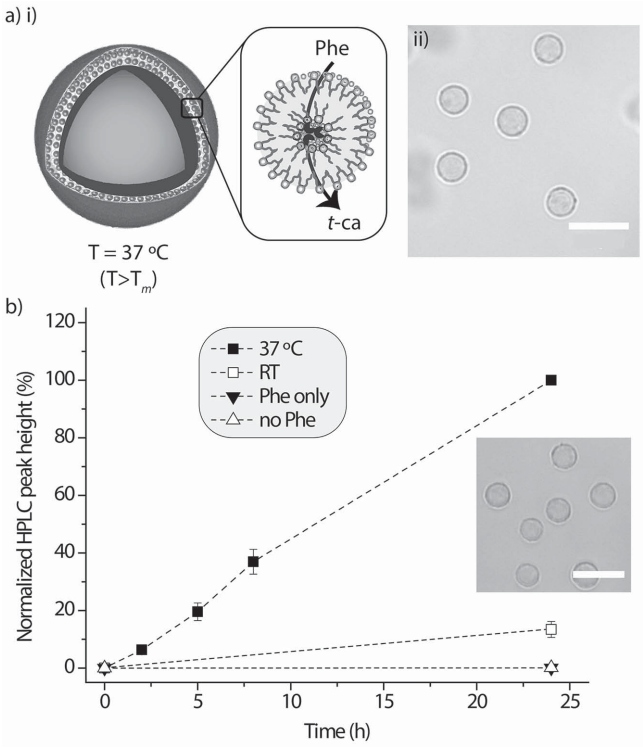

Figure 1. Characterization of PAL-loaded capsosomes. a-i) Schematic illustration of PDA-based capsosomes encapsulating the PAL enzyme within the liposomes. When increasing the *T* to 37 °C ($T > T_m$), the substrate Phe is able to cross the lipid membrane and to be converted into *t*-ca which is released from the compartment again. a-ii) DIC images of PAL-containing capsosomes. b) Reaction kinetics of PAL-loaded capsosomes incubated at 37 °C ($T > T_m$) (black squares) and at RT ($T < T_m$) (white squares) in the presence of Phe. As controls, PAL-loaded capsosomes were incubated in the absence of Phe (white triangles) and the Phe substrate was incubated in the absence of capsosomes (black triangles) at 37 °C. DIC image of capsosomes after 24 h of reaction (inset). Scale bars are 10 µm.

2.1.2. Recycling of the Capsosomes

Similarly to biological cells which perform successive enzymatic reactions within their organelles, we previously demonstrated that capsosomes (microreactors without core) can also conduct consecutive enzymatic reactions within their liposomal compartments.[22c] This aspect is crucial in enzyme replacement therapy, since it is desired that the encapsulated PAL enzyme remains active for an extended period of time. It is not only difficult and expensive to obtain the required enzyme in a highly purified and nontoxic form, but it is also beneficial for the patient's compliance and comfort if the number of required administration doses is limited. To confirm that the enzymatic reaction could take place in a continuous manner, i.e., the entrapped enzyme could be recycled; we repeated the enzymatic conversion by replacing the product with fresh substrate over several cycles. The results were normalized to the HPLC peak

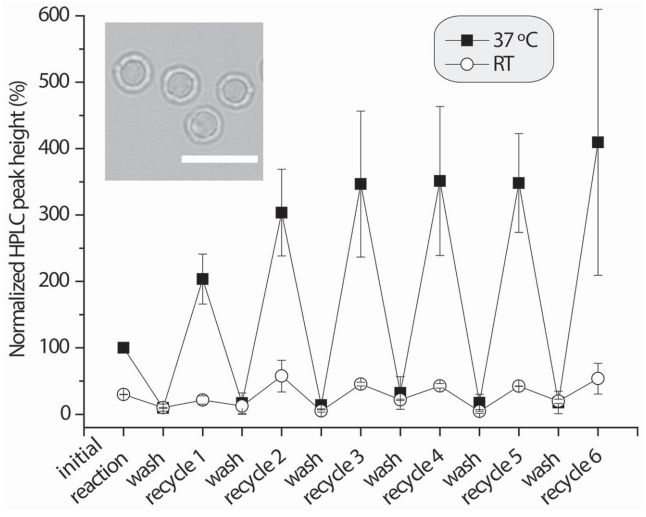

Figure 2. Enzymatic reaction in re-usable capsosomes. Normalized HPLC readings of the enzymatic assay of PAL-containing capsosomes incubated at RT (white circles) and at 37 °C (black squares). The enzymatic conversion was only observed when capsosomes were incubated at a higher T than the T_m of the liposomal subunits. DIC image of capsosomes after being re-used 6 × (inset). Scale bar is 10 μm.

height at 270 nm measured after the initial reaction at 37 °C. The enzymatic reaction occurred at a lowest rate for the initial reaction and the first cycle. After that, the enzymatic conversion occurred at a similar rate for all the tested subsequent cycles at 37 °C, while no *t*-ca was monitored in samples incubated at RT (**Figure 2**). These results indicated that the PAL enzyme was retained inside the liposomes, the enzymatic reaction could be reinitiated at least six times, and that there is no detectable loss of enzymatic activity. Additionally, capsosomes preserved their structural integrity after the 6 cycles (Figure 2, inset).

2.1.3. Stability over Time

Apart from ensuring that capsosomes can perform the enzymatic conversion in a continuous manner, understanding their stability over time for storage purposes is crucial. It is desired for any drug delivery system, that the activity is preserved for a known amount of time. With the aim to identify for how long the microreactors (with and without core) could be stored in solution without suffering loss of enzymatic activity, we prepared seven aliquots containing the same amount of microreactors (with and without core) in phosphate buffer (10×10^{-3} M, pH 8) and stored them at 4 °C. The enzymatic reaction was conducted in subsequent days using the different aliquots. Phe (at a final concentration of 6×10^{-6} M) was added before initiating the reaction which was triggered by incubating the aliquots at 37 °C. After 3 h, the aliquots were spun down (100 g, 30 s or 1680 g, 3 min for microreactors with and without core, respectively) and the supernatant was analyzed using HPLC by measuring the height of the absorbance peak of *t*-ca at 270 nm (**Figure 3**, black circles and black squares for microreactors with and without core, respectively). Controls incubated at RT were conducted in parallel (Figure 3, white circles and white squares for microreactors with and without core, respectively). The activity of PAL encapsulated within the microreactors slightly decreased for the first three days (i.e., a 30% and a 10% decrease in enzymatic activity was observed for microreactors with and without core, respectively). A significant loss of enzymatic activity was observed for microreactors with and without core after 5–6 d of storage in solution (i.e., on day 6, ≈70% of the enzymatic activity has been lost for both types of microreactor). These results suggested that microreactors with and without core can be stored in solution at 4 °C for a maximum of 4 d. DIC images of microreactors with and without core (Figure 3, inset, top, and bottom, respectively) demonstrate that the samples were intact and nonaggregated after being stored for 7 d. We speculate that the loss in activity was either due to the leakage of the enzymes or due to enzyme denaturation/degradation within the void of the liposomes over time.

Since the silica core did not negatively affect the performance of the encapsulated PAL enzyme, due to the reduced complexity in assembly and superior properties (i.e., absence of aggregation), the subsequent experiments were performed using capsosomes with core only. Importantly, the silica core

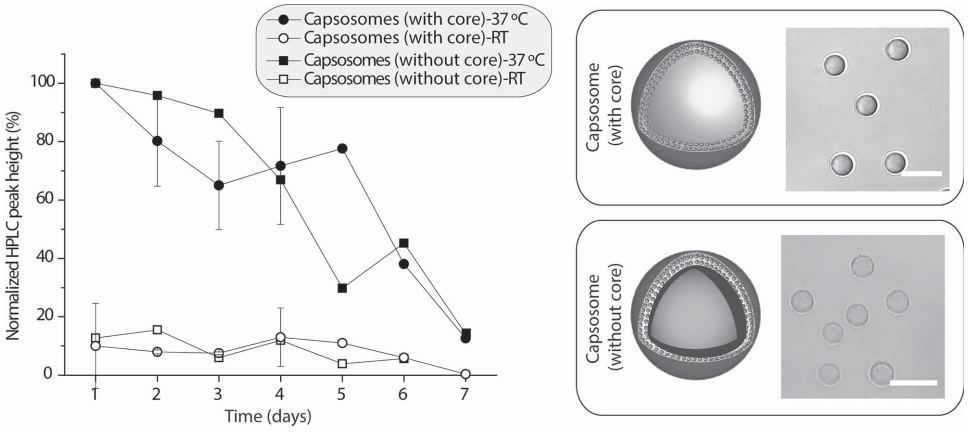

Figure 3. Normalized HPLC readings of enzymatic assays performed at 37 °C of microreactors with and without core (black circles and black squares, respectively) stored at 4 °C for several days. Controls in which the enzymatic reaction was performed at RT for microreactors with and without core (white circles and white squares, respectively) were performed in parallel. Representative DIC images of microreactors with (top) and without core (bottom) after being stored for 7 d. Scale bars are 10 μm.

is not expected to interfere with their envisioned application to be used as an oral formulation to treat PKU.

2.2. Microreactor Interaction with Cells

Since artificial cells are expected to be a powerful tool in biomedical applications such as drug delivery, we have previously assessed the interactions of capsosomes with several cell lines, focusing on internalization and cell viability.[23] In order to deplete Phe from the body, the microreactors will have to conduct the enzymatic reaction in the intestine, avoiding internalization by the cells lining the intestine wall. Therefore, understanding the interactions of the microreactors with human intestinal epithelial HT-29 cells is central.

To study this aspect, we employed three different concentrations of microreactors (N1 = 12.3 × 10^6 particles, N2 = 2 × N1, N3 = 3 × N1) containing fluorescently labeled liposomes. Confocal laser scanning microscopy (CLSM) images of the microreactors showed that they were nonaggregated and the liposomes were homogeneously distributed around the silica particle as indicated by the homogenous fluorescence signal (**Figure 4**a). We monitored the cell mean fluorescence (CMF) of the cells by flow cytometry after 3 h of incubation with the microreactors in 24 well-plates. (Please note that the autofluorescence of the cells was subtracted for all the shown results.) The results showed that there was no significant increase in CMF when increasing the concentration of the microreactors, indicating that already the lowest concentration saturated the cells with either internalized or membrane-associated particles (Figure 4b).

Next, since once reaching the intestine, the microreactors will be exposed to a low shear stress produced by the intestinal fluids and to a cyclic strain due to the peristalsis-like motions, we aim to mimic the dynamic in vivo environment in the intestine by applying peristaltic flow conditions to the cultured cells.

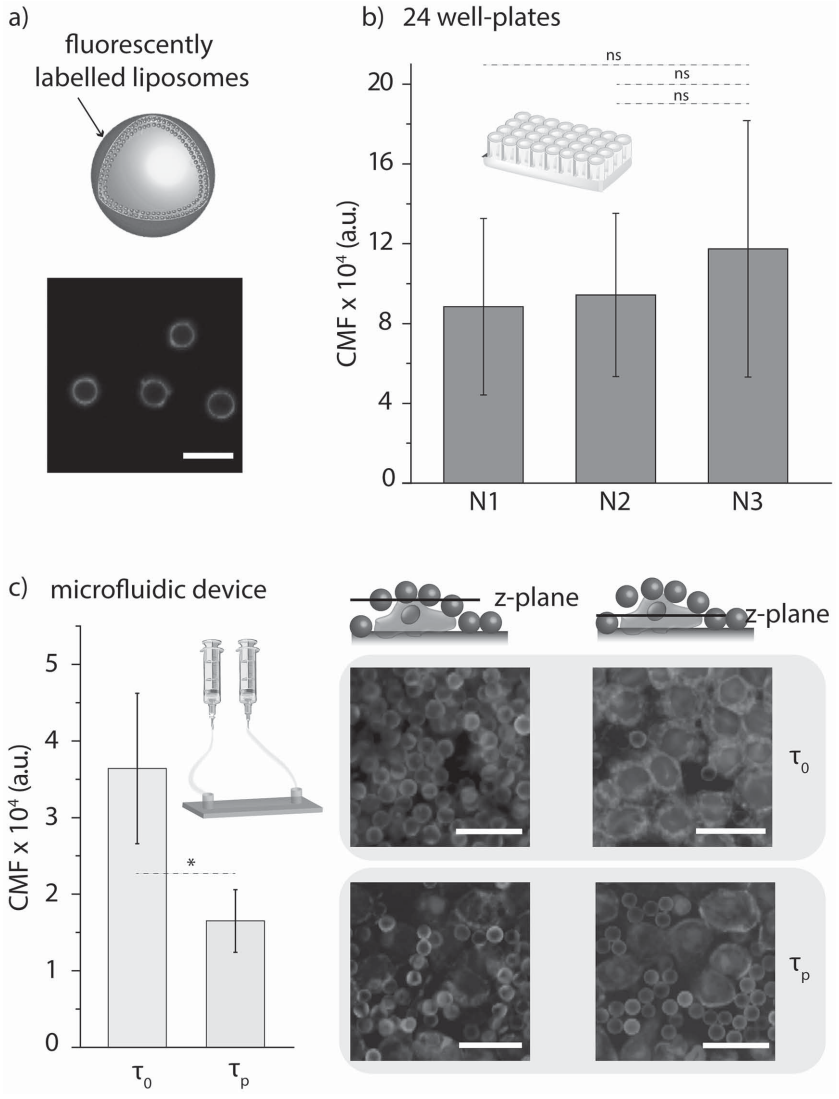

Figure 4. Microreactor interaction with cells. a) CLSM images of mircoreactors containing fluorescently labeled liposomes. Scale bar is 10 μm. b) Cell mean fluorescence (CMF) of HT-29 cells associated with microreactors containing fluorescently labeled liposomes at three different amounts (N1 = 12.3 × 10^6 particles, N2 = 2 × N1, N3 = 3 × N1) after 3 h of incubation in 24 well-plates. c) CMF of HT-29 cells associated with microreactors containing fluorescently labeled liposomes in the absence (τ_0) or presence (τ_p) of a peristaltic flow generated by means of a microfluidic device. ($n = 3$, * $p < 0.05$.) CLSM images of fixed HT-29 cells exposed to microreactors at τ_0 (top images) and τ_p (bottom images). The images were taken at a two different *z*-planes: on the top of the cells (left side images) and at the bottom of the sample (right side images). The cell nuclei and actin filaments were stained. Scale bars are 50 μm.

We studied the cell association/uptake of the microreactors by employing a microfluidic setup in which we recreated the intestinal flowing fluid by applying a low shear stress (0.24 dyn cm^{-2}) over the microchannel and by exerting a cyclic strain (0.15 Hz) that mimics the physiological peristalsis-like motions.[24] We would like to note that the employed shear stress was 10× higher due to practical reasons than the physiological one (0.02 dyn cm^{-2}). This microfluidic set up (Scheme 1b) better mimics the environment the microreactors will experience in the intestine when interacting with the cells than when cultured in a static well-plate model. Figure 4c depicts the CMF of HT-29 cells upon exposure to microreactors containing fluorescently labeled liposomes in the microfluidics device in the presence (τ_p) or absence (τ_0) of peristaltic flow. The results indicated that at τ_p, the amount of microreactors associated/internalized by the cells was significantly decreased. We speculate that upon application of τ_p some of the microreactors get washed away and/or the residence time of the microreactors on the cell membrane was decreased or altered, and therefore, the association/uptake was lowered. To verify that the microreactors were not internalized but associated with the cell membrane,

the cell nuclei and actin filaments were stained and the samples were examined by CLSM. Figure 4c shows a representative CLSM image of fixed HT-29 cells exposed to microreactors at τ_0 (top) and τ_p (bottom). The images on the left side correspond to a *z*-plane on top of the cells while the images on the right correspond to a *z*-plane of the bottom of the sample. It could be observed that the microreactors remained outside the cells for τ_0 and τ_p, confirming that the vast majority of the microreactors were not internalized by the cells. The CLSM images at τ_0 (Figure 4c, top right) revealed internalization of the fluorescent lipids from the microreactors by the cells (as shown by the brighter fluorescence intensity of the cells), explaining the higher CMF measured by flow cytometry. It is interesting to note that upon application of τ_p, the amount of internalized fluorescent lipids was lower, which is favorable for our application in mind. We have previously reported the assembly of liposome containing PDA films and evaluated their potential in surface-mediated drug delivery where we showed that different cells can internalize fluorescent lipids from the surface.[25] In this current study, we demonstrated that fluorescent lipids could also be internalized from liposomes within a PDA coating by cells when administered from the top. This fact could be of interest to deliver hydrophobic cargo from a solution-based drug delivery perspective.

2.3. Enzymatic Reaction of Microreactors in the Presence of Cells

Since liposome containing microreactors will have to conduct the enzymatic reaction in the intestine, assessing the activity of the PAL-loaded microreactors in the presence of cells is another key aspect to address. In general, only few published reports have considered the biological environment when performing encapsulated biocatalysis, focusing on intracellular activity. Hunzinker and co-workers were the first ones to report encapsulated enzymatic activity inside of cells.[26] They reported the design and assembly of nano-sized polymer vesicles which were subsequently loaded with the enzyme trypsin. The polymer vesicles were internalized into macrophages and an enzymatic reaction in which a specific substrate was converted into a fluorescent product was performed intracellularly. Follow up work on encapsulated enzymatic reactions performed intracellularly remain scarce[8a,27] and, to the best of our knowledge, none of the multicompartment systems reported to date has shown encapsulated enzymatic activity in the presence of cells. Since, our goal is to deplete Phe from the intestinal lumen; therefore, our microreactors should and are not being internalized by the human intestinal cells. Herein, we advance the artificial cell concept by performing, for the first time, an enzymatic reaction extracellularly.

We first assessed the enzymatic conversion of Phe by several concentrations of PAL-containing microreactors in the presence of cells and in PBS as a control in 24 well-plates. We incubated different amounts of microreactors (N1 = 12.3×10^6 particles, N2 = 2 × N1, N3 = 3 × N1) for 3 h at a final concentration 6×10^{-6} M of Phe in 24 well-plates in the presence of cells (and full cell media) or in PBS. After the incubation time, the supernatant was removed and analyzed by HPLC. The height of the absorbance peak at 270 nm corresponding to *t*-ca was measured. Upon increasing the concentration of particles, the signal corresponding to *t*-ca also increased (**Figure 5**a). Interestingly, for the same amount of particles, no significant differences in

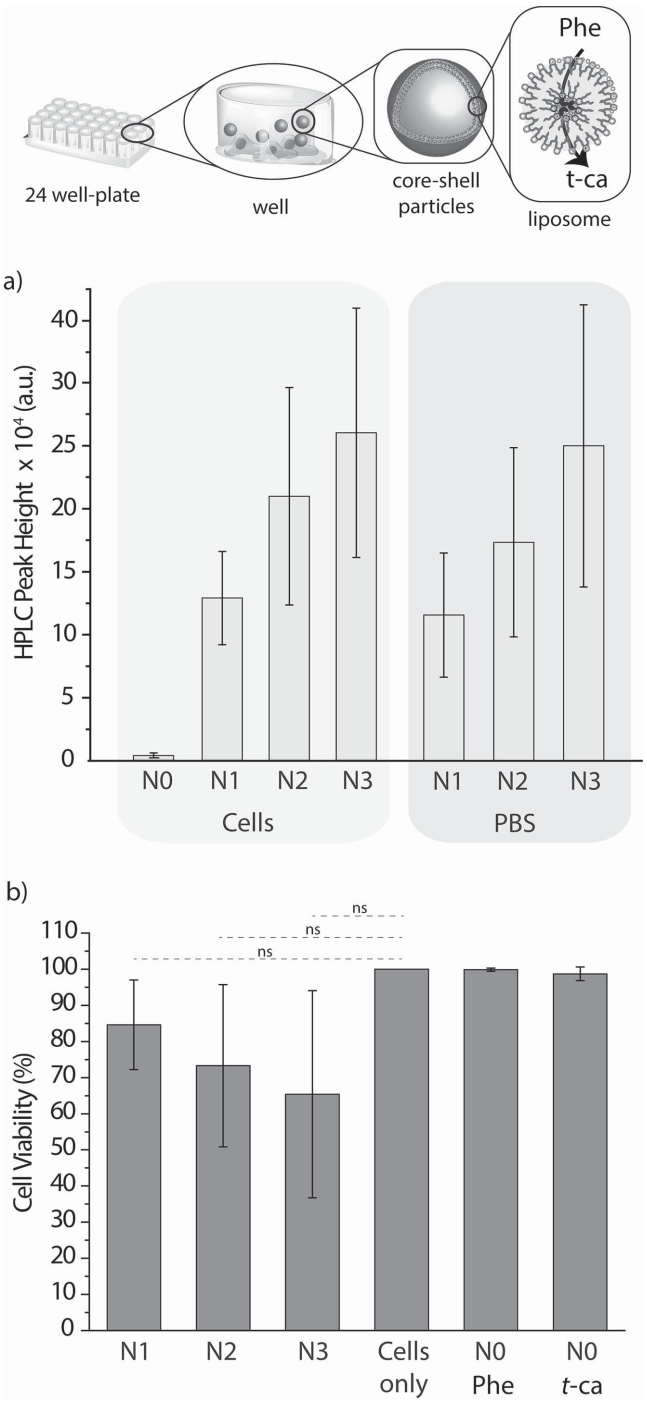

Figure 5. a) Enzymatic conversion of Phe into *t*-ca by PAL-loaded microreactors at three different concentrations (N1 = 12.3×10^6 particles, N2 = 2 × N1, N3 = 3 × N1) incubated in the presence of HT-29 cells (and full cell media) or in PBS for 3 h. b) Normalized cell viability of HT-29 cells after conducting the encapsulated enzymatic reaction for 3 h. The results have been normalized to cells incubated in cell media only ($n = 3$, * $p < 0.05$).

t-ca peak height were observed for particles incubated in the presence of cells or in PBS. This fact demonstrates that the presence of cells did not negatively affect the PDA membrane or the liposomes encapsulating the enzymes, allowing for the equal performance of the microreactor in PBS and the biological environment. Next, a cytotoxicity assay was conducted with the aim to ensure that neither the microreactors nor the enzymatic reaction impaired the cell viability. Figure 5b shows that there was no significant decrease in cell viability after performing the enzymatic reaction for 3 h at the three employed amounts of microreactors, confirming the absence of inherent cytotoxicity in our approach. Importantly, there was also no decrease in cell viability for cells incubated in the presence of 6×10^{-6} M Phe or 10×10^{-6} M *t*-ca, demonstrating that neither the substrate or the product of the enzymatic reaction are cytotoxic at the reported concentrations.

We next aimed to assess the enzymatic performance of the microreactors at τ_p, to confirm that neither the shear stress nor the cyclic strain did damage the polymer membrane or the liposomes. By doing so, the PAL-containing microreactors were tested for their ability to conduct the enzymatic reaction after being exposed to a dynamic environment similar to the one they will encounter in the intestine. N1 microreactors were placed in the channel of the microfluidic set up with preseeded cells, and τ_p was applied for 3 h, since the mean residence time in the small intestine ranges from 2–5 h.[9] Next, Phe at a final concentration of 6×10^{-6} M was added to the channels and allowed to incubate for an extra 3 h at τ_0. As controls, the enzymatic reaction at τ_0 was performed in a channel containing preseeded cells with N1 microreactors, in a channel containing preseeded cells without microreactors, and in a channel containing microreactors incubated in PBS without preseeded cells. The supernatant was removed from the channels and injected into the HPLC. The height of the peak corresponding to *t*-ca at 270 nm was measured. There was no significant difference in peak height when comparing the amount of *t*-ca produced by microreactors at τ_p compared to τ_0. As expected, there was no *t*-ca conversion when no microreactors were added to the sample (N0) and, importantly, there was no significant difference in the amount of converted *t*-ca when N1 microreactors where incubated at τ_0 and in the absence of cells (**Figure 6**a). These results confirm that neither the presence of cells nor the peristaltic flow applied had a significant influence in the microreactor performance. A cytotoxicity assay was also conducted after performing the enzymatic reaction, confirming that neither the peristaltic flow applied for 3 h nor the enzymatic reaction conducted afterward diminished the cell viability (Figure 6b). These results demonstrated, for the first time, the successful extracellular activity of an enzymatic microreactor in a dynamic environment.

Additionally, we assessed if the enzymatic reaction could take place while applying the peristaltic flow. N2 microreactors were placed in the channel of the microfluidic set up. Full cell media containing Phe to a final concentration of 0.6×10^{-3} M was placed in the syringe reservoirs. τ_p was applied for 3 h. A control without the peristaltic flow (τ_0) was conducted in parallel. After the required incubation time, the cell media from the reservoirs was freeze-dried, resuspended in PBS and injected into the HPLC. The height of the peak measured at 270 nm corresponding to *t*-ca demonstrates that the enzymatic reaction can also take place while peristaltic flow is applied (Figure S1, Supporting Information).

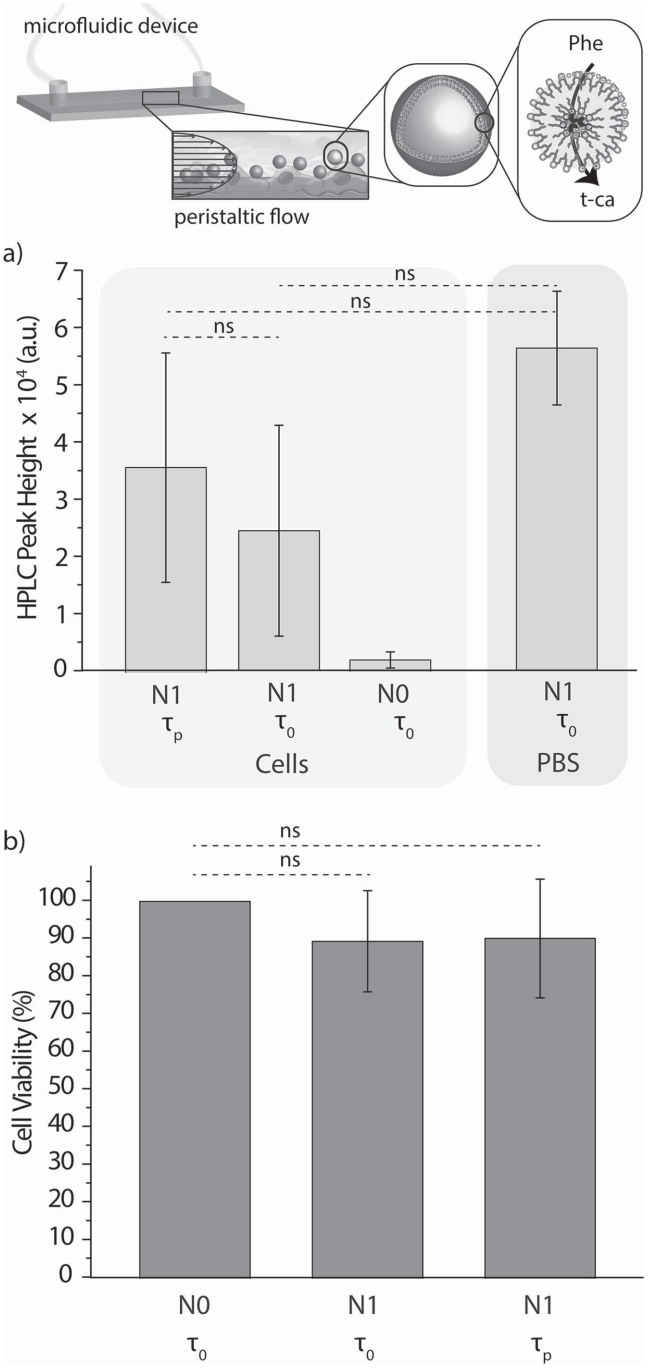

Figure 6. a) Enzymatic conversion of Phe into *t*-ca by PAL-loaded microreactors (N1 = 12.3×10^6 microreactors) incubated in the presence of HT-29 cells (and full cell media) or in PBS for 3 h after the presence (τ_p) or absence (τ_0) of peristaltic flow for 3 h. b) Normalized cell viability of HT-29 cells after conducting the aforementioned encapsulated enzymatic reaction at τ_p or τ_0. The results have been normalized to cells incubated in the perfusion chamber at τ_0.

3. Conclusion

We have demonstrated that liposome containing microreactors were able to perform an encapsulated enzymatic reaction in the presence of cells after and while being exposed to peristaltic flow which mimics the dynamic environment that the microreactors will experience in the intestine. The results therefore represent a significant step toward a functional artificial cell. Although several challenges still remain to be addressed such as the stability and functional performance of microreactors in GI fluids, we, for the first time, have moved on from model enzymes to encapsulating a therapeutic enzyme and demonstrating the potential of our microreactors toward the treatment of a medical condition, i.e., the treatment of PKU.

4. Experimental Section

Materials: Poly(L-lysine) ($\bar{M}_w$ 40 000–60 000), dopamine hydrochloride, sodium chloride (NaCl), tris(hydroxymethyl)aminomethane (TRIS), phenylalanine (Phe), *trans*-cinnamic acid (*t*-ca), ammonium fluoride, HF, sodium phosphate dibasic, sodium phosphate monobasic, paraformaldehyde, Triton X-100, 4′,6-diamidino-2-phenylindole (DAPI), phalloidin, chloroform, acetonitrile (MeCN), methanol, trifluoroacetic acid (TFA), pancreatin, and bile salt mixture were purchased from Sigma-Aldrich. Silica particles (4.8 or 5.6 μm diameter) were purchased from Microparticles GmbH, Germany. Zwitterionic lipids, 1,2-dimyristoyl-*sn*-glycero-3-phosphocholine (DMPC, phase transition temperature 24 °C), 1,2-dipalmitoyl-*sn*-glycero-3-phosphocholine (DPPC, phase transition temperature 41 °C), and fluorescent lipids 1-oleoyl-2-[6-[(7-nitro-2-1,3-benzoxadiazol-4-yl)amino]hexanoyl]-*sn*-glycero-3 phosphocholine (NBD-PC) were purchased from Avanti Polar Lipids, USA. Poly(methacrylic acid)-*co*-(cholesteryl methacrylate) (PMA_c, $\bar{M}_w$ 33 kDa) was synthesized according to a previously published protocol.[28] Histidine-tagged variant of the Anabaena variabilis PAL enzyme, bearing C503S, C565S and F18A point mutations were expressed and purified based on the protocols described in our previous publication.[29] Water from the Millipore water system (Milli-Q gradient A 10 system, resistance 10 MΩ cm, TOC < 4 ppb, Millipore Corporation, USA) was used for all the experiments.

Liposome Formation: Unilamellar zwitterionic liposomes were prepared by evaporation of the chloroform of the lipid solution (2.5 mg) under nitrogen for 1 h, followed by hydration with 1 mL of TRIS buffer (TRIS 100×10^{-3} M, pH 7.0) at 37 °C containing 0.5 mg of the PAL enzyme. For fluorescently labeled liposomes, 6 wt% of NBD-PC was added to the lipid solution. Each solution was extruded through 200 nm filters 11 × followed by an extrusion through 100 nm filters. The extrusion was performed at 37 °C. Liposomes with sizes of ≈120 nm were obtained.

Capsosome Assembly: A suspension of SiO_2 particles (5 wt%) TRIS buffer was incubated with the polymer precursor layer, PLL (1 mg mL^{-1}, 10 min), and washed three times in TRIS buffer (100 g, 30 s) followed by the adsorption of a PMA_c layer (0.7 mg mL^{-1}, 10 min), washed 3× in TRIS buffer and suspended in a liposome solution (2.5 mg mL^{-1}, 50 min, 37 °C), washed 3× in TRIS and incubated in a PMA_c solution again (0.7 mg mL^{-1}, 15 min, 37 °C), washed 3× in TRIS, followed by the absorption of a second liposome deposition step (2.5 mg mL^{-1}, 50 min). The samples were then washed 3× in TRIS followed by the adsorption of a PMA_c capping layer (0.7 mg mL^{-1}, 15 min, 37 °C). When employing fluorescent lipids, the samples were covered with aluminum foil to avoid the exposure of the fluorescent dyes to light and possible photobleaching. After absorbing the PMA_c capping layer, the core-shell particles were washed 3× in a TRIS solution (10×10^{-3} M, pH 8.5) and the PDA shell was deposited by incubating them in a dopamine solution (8 mg mL^{-1} in a TRIS solution (10×10^{-3} M, pH 8.5)) for ≈16 h. After the incubation time, the particles where washed 3× in a TRIS solution (TRIS 10×10^{-3} M, 150×10^{-3} M NaCl, pH 7.4). For capsosomes without core, silica particles were dissolved using a 2 M HF/8 M ammonium fluoride (NH_4F) solution at pH 5 for 2 min, followed by multiple centrifugation (1680 g, 5 min) washing cycles in Milli-Q. Since in our previous report we employed unsaturated liposomes for the PDA-capsosomes assembly,[21] to confirm the adsorption of liposomes composed of saturated lipids (DMPC/DPPC) in the new PDA-capsosomes, we monitored the capsosomes assembly on colloids by flow cytometry employing fluorescently labeled liposomes (Figure S2, Supporting Information). The results demonstrate that two layers of liposomes could be deposited and that the second liposome deposition step contained ≈5× more liposomes than the first one, results that are in agreement with our previous, in which a higher liposomal loading was also achieved in the second liposome deposition step.[21]

Dynamic Light Scattering (DLS): The size and polydispersity (PD) of the liposomes was determined by diluting 30–50 μL of sample solution in ≈700 μL of MQ prior to measuring in a DLS instrument (Zeta-sizer nano, Malvern Instruments) using a material refractive index of 1.590 and a dispersant (water at 25 °C) refractive index of 1.330. Liposomes were found to have a diameter ≈120 nm with a PD < 0.15.

Differential Interference Contrast (DIC) Microscopy: DIC images of capsosomes with or without core were taken with an inverted Zeiss microscope Axio Observer Z1 (Zeiss, Germany) equipped with a DIC slider, the corresponding filter sets and a 63× oil immersion objective.

Confocal Laser Scanning Microscopy: Microreactors containing fluorescently labeled liposomes were imaged with an Axiovert microscope coupled to an LSM 700 confocal laser scanning module (Zeiss, Germany).

Flow Cytometry: The number of capsosomes (with or without core) was quantified by flow cytometry using a BD Accuri C6 flow cytometer. At least 10 000 particles were analyzed in each experiment and at least two independent experiments were performed.

Enzymatic Reactions: Kinetics of Enzymatic Conversion of Phe: 100 μL of a suspension containing 9.9×10^4 capsosomes loaded with PAL-containing liposomes was allowed to interact with a solution 6×10^{-6} M of Phe in phosphate buffer (10×10^{-3} M, pH 8) at 37 °C or at RT (23 °C). The conversion of Phe into *t*-ca was measured by spinning down the capsosomes (1680 g, 3 min) and 90 μL of the supernatant were injected in a HPLC.

Cycling of the Enzymatic Conversion of Phe: 110 μL of a 2.8×10^7 capsosome suspension containing Phe (6×10^{-6} M in phosphate buffer (10×10^{-3} M, pH 8)) was incubated at RT (23 °C) or 37 °C for 1 h. The absorbance readings were monitored over time at 270 nm via HPLC. The capsosomes were centrifuged (1680 g, 3 min), and the supernatant (containing *t*-ca) was removed and replaced by fresh Phe solution, followed by incubation at a given temperature and HPLC measurement (90 μL).

Stability over Time of PAL-Containing Microreactors: 7 aliquots of 110 μL suspensions of 12×10^6 microreactors (with or without core) in phosphate buffer (10×10^{-3} M, pH 8) were stored over days at 4 °C. Each day one aliquot was incubated at 37 °C for 3 h with Phe 6×10^{-6} M. The microreactors were centrifuged (100 *g*, 30 s, (with core) or 1680 g, 3 min (without core)) and 90 μL of the supernatant were injected into the HPLC to monitor the *t*-ca conversion at 270 nm. Analytical HPLC was performed on a Shimazdu LC-2010A HT system equipped with an Ascentis Express Peptide ES-C18 column with 2.7 μm particles, a length of 15 cm and an internal diameter of 3.0 mm from Supelco. The product *t*-ca was identified at $\lambda = 270$ nm. The system was run at a flow rate of 4.0 mL min^{-1}, 90 μL of injection and a gradient = 0%–2% B for 5 min, 2%–35% B for 3 min and 35%–55% for 12 min (A = 0.045% TFA in H_2O and B = 0.05% TFA in MeCN).

Cell Experiments: The HT-29 human colorectal adenocarcinoma cell line (ATTC) was used for all the experiments. The cells (1 000 000 cells per flask in 20 mL of media) were cultured in 75 cm^2 culture flasks in media (McCOY'S 5A with $NaHCO_3$ supplemented with 10% fetal bovine serum, 2×10^{-3} M glutamine, 50 μg mL^{-1} penicillin, 50 μg mL^{-1} streptomycin, all purchased from Sigma-Aldrich) at 37 °C and 5% CO_2. To perform 3 h long continuous flow experiments, cells were seeded at

a density of 1 000 000 cells per channel in 300 µL media into closed perfusion chambers (µ-slide I 0.8 Luer, tissue culture treated, Ibidi GmbH, Munich, Germany) and at a density of 500 000 cells per well in 0.5 mL of media onto a 24-well plate and allowed to attach for 24 h at 37 °C and 5% CO_2.

Cell Association/Uptake Experiments: 24 Well-Plates: 300 µL cell media containing microreactors with fluorescently labeled liposomes at three different concentrations (N1 = 12.3×10^6, N2 = 24.6×10^6, and N3 = 36.9×10^6 particles) were added to the wells and incubated for 3 h.

Microfluidic Set-Up: 300 µL media containing microreactors with fluorescently labeled liposomes at a concentration N1 = 12.3×10^6 particles was added to the channel. 12 mL media was added to the reservoir (syringe) of the commercial ibidi pumping system (Ibidi GmbH, Munich, Germany) as depicted in Scheme 1b. The perfusion chamber was connected to a first fluidic unit to create a unidirectional flow (with a shear stress of 0.24 Pa) followed by a second fluidic unit which periodically interrupted to create a pulsation of 0.15 Hz (τ_p). Both fluidic units and the perfusion chambers were placed in the incubator (37 °C and 5% CO_2). As controls, 300 µL media containing sample and 300 µL media without sample were added to two perfusion chambers not connected to the fluidic units (i.e., static conditions, τ_0). The perfusion chambers were incubated for 3 h. After the 3 h incubation time, the wells or channels were washed with PBS (200 µL) 2×, followed by the addition of trypsin (200 µL, 5 min) to detach the cells. The cells were harvested by washing the wells or channels with PBS (200 µL) 2× and analyzed by flow cytometry. The autofluorescence of the cells was subtracted in all present results by subtracting the CMF of cell cultured in the absence of any microreactors from the cells cultured in the presence of the microreactors. At least 3000 cells were analyzed. For fluorescence imaging, the HT-29 cells were washed with PBS (200 µL) 2× and fixed using a 4% paraformaldehyde solution for 20 min followed by multiple PBS washing steps. For staining, the cells were permeabilized using T-PBS (0.1% Triton X-100 in PBS, 15 min) and their nuclei and actin filaments were stained by incubating them in a solution of 4',6-diamidino-2-phenylindole (DAPI, 2.5 µg mL^{-1}) and phalloidin (0.1 µg mL^{-1}) in PBS for 1 h. The samples were washed 3× with T-PBS and 1× in PBS. The images were taken with a confocal laser scanning microscope (LSM 710, Zeiss, Germany).

Enzymatic Reactions: 24 Well-Plates: 300 µL cell media or PBS containing microreactors with PAL-loaded liposomes at three different concentrations (N1 = 12.3×10^6 particles, N2 = 2 × N1 and N3 = 3 × N1) were added to the wells and incubated for 3 h.

Microfluidic Set-Up: 300 µL media containing microreactors with PAL-loaded liposomes at a concentration N1 = 12.3×10^6 particles was added to the channel. The same procedure was followed as previously described for the cell association/uptake experiments. As controls, 300 µL of media containing sample and 300 µL of media without sample and 300 µL of PBS containing sample were added to three perfusion chambers not connected to the fluidic units (i.e., static conditions). The perfusion chambers were incubated for 3 h. After the incubation time, 5 µL Phe (5 mg mL^{-1} in PBS) or *t*-ca (1 mg mL^{-1} in PBS) were added to the wells or channels and allowed to incubate for 3 h in static conditions (i.e., without the fluidic units). Following incubation, the supernatant was removed and passed through a centrifugation filter (MWCO 3k, 14 000 rcf, 25 °C, 30 min) prior to injection into the HPLC. For the enzymatic reaction under peristaltic flow, 300 µL media containing PAL-loaded microreactors at a concentration of N2 = 24.6×10^6 particles were added to the channel. 12 mL media containing Phe at a concentration 0.1 mg mL^{-1} was added to the reservoir (syringe) of the pumping system. The peristaltic flow was applied as previously described for 3 h. After the incubation time, the cell media was removed from the chambers and reservoirs, passed through a centrifugation filter (MWCO 3k, 14 000 rcf, 25 °C, 30 min) and freeze-dried. The lyophilized powder was resuspended in 200 µL PBS and injected into the HPLC.

Cell Viability: For the cell viability experiments, the channels and the wells were flush washed with PBS (200 µL) 2× and cell media (200 µL) 1× followed by adding 200 µL of a mixture containing 180 µL of cell media and 20 µL of the assay cell solution Cell Counting Kit-8 (Doijindo) to each channel or well for 2 h at 37 °C and 5% CO_2. After incubation, 200 µL of the cell media/counting kit mixture were transferred to a 96-well plate and the absorbance at 460 nm was monitored using a multimode plate reader (PerkinElmer). All cell experiments were performed in three independent repeats. The statistical significance (*p* value) used to compare the distribution of samples was determined using a 1-way ANOVA with a confidence level of 95% ($\alpha = 0.05$), followed by a Tukey's multiple comparison post hoc test. (* = $p < 0.05$, ** = $p < 0.01$, *** = $p < 0.001$.)

Supporting Information

Supporting Information is available from the Wiley Online Library or from the author.

Acknowledgements

This work was supported by a Marie Curie individual fellowship (L. H-R.) and the Carlsberg foundation, Denmark. The authors thank Associate Prof. R. Meyer (iNANO, Aarhus University, Denmark) for access to the CLSM, and Associate Prof. A. Zelikin (Department of Chemistry, Aarhus University, Denmark) for access to the DLS, plate reader, flow cytometer, HPLC and microscope. The authors gratefully acknowledge Dr. P. Ruiz-Sanchis and B. M. Wohl (Department of Chemistry, Aarhus University, Denmark) for the assistance in the *t*-ca detection by HPLC.

Received: November 25, 2014
Revised: April 29, 2015
Published online: May 26, 2015

[1] N. Blau, A. Belanger-Quintana, M. Demirkol, F. Feillet, M. Giovannini, A. MacDonald, F. K. Trefz, F. van Spronsen, P. K. U. C. Contributing European, *Mol. Genet. Metab.* **2010**, *99*, 109.
[2] W. Kim, H. Erlandsen, S. Surendran, R. C. Stevens, A. Gamez, K. Michols-Matalon, S. K. Tyring, R. Matalon, *Mol. Ther.* **2004**, *10*, 220.
[3] a) I. Smith, *Arch. Dis. Child.* **1993**, *68*, 426.
[4] a) R. C. Eisensmith, S. L. C. Woo, *Eur. J. Pediat.* **1996**, *155*, S16; b) Z. B. Ding, C. O. Harding, B. Thony, *Mol. Genet. Metab.* **2004**, *81*, 3.
[5] a) M. J. MacDonald, G. B. D'Cunha, *Biochem. Cell Biol.* **2007**, *85*, 273; b) C. N. Sarkissian, A. Gamez, *Mol. Genet. Metab.* **2005**, *86*, S22.
[6] J. A. Hoskins, J. Gray, *Res. Commun. Chem. Pathol. Pharmacol.* **1982**, *35*, 275.
[7] a) A. Pisani, B. Visciano, G. D. Roux, M. Sabbatini, C. Porto, G. Parenti, M. Imbriaco, *Mol. Genet. Metab.* **2012**, *107*, 267; b) A. Toscano, B. Schoser, *J. Neurol.* **2013**, *260*, 951; c) V. Valayannopoulos, *Handb. Clin. Neurol.* **2013**, *113*, 1851.
[8] a) C. De Vocht, A. Ranquin, R. Willaert, J. A. Van Ginderachter, T. Vanhaecke, V. Rogiers, W. Versees, P. Van Gelder, J. Steyaert, *J. Controlled Release* **2009**, *137*, 246; b) S. M. Rombach, C. E. M. Hollak, G. E. Linthorst, M. G. W. Dijkgraaf, *Orphanet J. Rare Dis.* **2013**, *8*, 29.
[9] G. Fuhrmann, J.-C. Leroux, *Pharm. Res.* **2014**, *31*, 1099.
[10] C. W. Abell, R. S. Shen, *Methods Enzymol.* **1987**, *142*, 242.
[11] H. J. Gilbert, M. Tully, *Biochem. Biophys. Res. Commun.* **1985**, *131*, 557.
[12] T. M. S. Chang, L. Bourget, C. Lister, *Artif. Cells, Blood Substitues, Immobilization Biotechnol.* **1995**, *23*, 1.

[13] T. M. S. Chang, *Nat. Rev. Drug Discovery* **2005**, *4*, 221.
[14] J. M. Harris, R. B. Chess, *Nat. Rev. Drug Discovery* **2003**, *2*, 214.
[15] K. J. Wieder, N. C. Palczuk, T. Vanes, F. F. Davis, *J. Biol. Chem.* **1979**, *254*, 2579.
[16] S. Frokjaer, D. E. Otzen, *Nat. Rev. Drug Discovery* **2005**, *4*, 298.
[17] X. L. Wang, J. Y. Shao, *Biomater., Artif. Cells, Immobilization Biotechnol.* **1993**, *21*, 637.
[18] a) M. Marguet, C. Bonduelle, S. Lecommandoux, *Chem. Soc. Rev.* **2013**, *42*, 512; b) L. Hosta-Rigau, B. Stadler, in *Regenerative Medicine, Artificial Cells and Nanomedicine, Selected Topics in Nanomedicine*, Vol. 3 (Ed: T. M. S. Chang), World Science Publisher/Imperial College Press, McGill University, Canada **2013**.
[19] B. M. Teo, L. Hosta-Rigau, M. E. Lynge, B. Stadler, *Nanoscale* **2014**, *6*, 6426.
[20] H. J. Gilbert, G. W. Jack, *Biochem. J* **1981**, *199*, 715.
[21] L. Hosta-Rigau, M. J. York-Duran, Y. Zhang, K. N. Goldie, B. Stadler, *ACS Appl. Mater. Interfaces* **2014**, *6*, 12771.
[22] a) B. Städler, R. Chandrawati, A. D. Price, S.-F. Chong, K. Breheney, A. Postma, L. A. Connal, A. N. Zelikin, F. Caruso, *Angew. Chem. Int. Ed.* **2009**, *48*, 4359; b) L. Hosta-Rigau, B. Stadler, Y. Yan, E. C. Nice, J. K. Heath, F. Albericio, F. Caruso, *Adv. Funct. Mater.* **2010**, *20*, 59; c) R. Chandrawati, L. Hosta-Rigau, D. Vanderstraaten, S. A. Lokuliyana, B. Stadler, F. Albericio, F. Caruso, *ACS Nano* **2010**, *4*, 1351; d) L. Hosta-Rigau, S. F. Chung, A. Postma, R. Chandrawati, B. Stadler, F. Caruso, *Adv. Mater.* **2011**, *23*, 4082.
[23] L. Hosta-Rigau, R. Chandrawati, E. Saveriades, P. D. Odermatt, A. Postma, F. Ercole, K. Breheney, K. L. Wark, B. Stadler, F. Caruso, *Biomacromolecules* **2010**, *11*, 3548.
[24] H. J. Kim, D. Huh, G. Hamilton, D. E. Ingber, *Lab Chip* **2012**, *12*, 2165.
[25] M. E. Lynge, M. Fernandez-Medina, A. Postma, B. Städler, *Macromol. Biosci.* **2014**, *12*, 1677.
[26] N. Ben-Haim, P. Broz, S. Marsch, W. Meier, P. Hunziker, *Nano Lett.* **2008**, *8*, 1368.
[27] a) S. F. M. van Dongen, W. P. R. Verdurmen, R. J. R. W. Peters, R. J. M. Nolte, R. Brock, J. C. M. van Hest, *Angew. Chem. Int. Ed.* **2010**, *49*, 7213; b) P. Tanner, O. Onaca, V. Balasubramanian, W. Meier, C. G. Palivan, *Chem. Eur. J.* **2011**, *17*, 4552; c) M. K. Reddy, V. Labhasetwar, *FASEB J.* **2009**, *23*, 1384.
[28] M. E. Lynge, M. B. Laursen, L. Hosta-Rigau, B. E. B. Jensen, R. Ogaki, A. A. A. Smith, A. N. Zelikin, B. Stadler, *ACS Appl. Mater. Interfaces* **2013**, *5*, 2967.
[29] L. Wang, A. Gamez, H. Archer, E. E. Abola, C. N. Sarkissian, P. Fitzpatrick, D. Wendt, Y. Zhang, M. Vellard, J. Bliesath, S. M. Bell, J. F. Lemontt, C. R. Scriver, R. C. Stevens, *J. Mol. Biol.* **2008**, *380*, 623.